Results in Physics 51 (2023) 106656

Contents lists available at ScienceDirect

Results in Physics

journal homepage: www.elsevier.com/locate/rinp

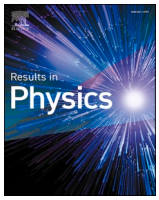

Performance investigations on integrated MMF/FSO transmission enabled by OAM beams

Mehtab Singh [a], Somia A. Abd El-Mottaleb [b], Syed Alwee Aljunid [c,d], Hassan Yousif Ahmed [e], Medien Zeghid [e,f], Kottakkaran Sooppy Nisar [g,*]

[a] Department of Electronics and Communication Engineering, University Institute of Engineering, Chandigarh University, Mohali, Punjab 140413, India
[b] Alexandria Higher Institute of Engineering and Technology, Alexandria 21311, Egypt
[c] Faculty of Electronic Engineering and Technology, Universiti Malaysia Perlis, Arau, Perlis 02600, Malaysia
[d] Centre of Excellence Advanced Communication Engineering (ACE), Universiti Malaysia Perlis, Arau, Perlis 02600, Malaysia
[e] Department of Electrical Engineering, College of Engineering in Wadi Alddawasir, Prince Sattam Bin Abdulaziz University, Wadi Alddawasir 11991, Saudi Arabia
[f] Electronics and Micro-Electronics Laboratory (E. μ. E. L), Faculty of Sciences, University of Monastir, Monastir 5000, Tunisia
[g] Department of Mathematics, College of Science and Humanities in Alkharj, Prince Sattam Bin Abdulaziz University, Alkharj 11942, Saudi Arabia

ARTICLE INFO

Keywords:
Multimode fiber (MMF)
Optical wireless communication (OWC)
Atmospheric turbulences
Bit error rate (BER)

ABSTRACT

This paper introduces a new hybrid system for high-bandwidth and high-transmission-capacity communication. The system integrates a multi-mode fiber (MMF) cable with free space optics (FSO) using orbital angular momentum (OAM) multiplexing. The proposed system uses a single wavelength to simultaneously transmit 40 Gb/s data on four distinct OAM beams ($LG_{0,0}$, $LG_{0,17}$, $LG_{0,40}$, and $LG_{0,75}$)) with a symmetric circular shape. The performance of the system was evaluated with a fixed MMF length of 100 m and varying FSO ranges, according to extreme climate changes such as rain and fog, and atmospheric turbulences. The results indicate that the suggested system is capable of transmit up to 1250 m (100 m MMF length + 1150 m FSO range) under clear weather (CW) and weak turbulence (WT), with a minimum transmission distance of 440 m (100 m MMF length + 340 m FSO range) under heavy fog (HF). The performance of the system was also demonstrated based on actual meteorological data for two different cities, Alexandria, Egypt and Chandigarh, India, with different visibility ranges and geographical locations. Since Alexandria has a longer visibility range than Chandigarh, our proposed model could spread over a larger area than it could be in Chandigarh. The obtained ranges were within an acceptable bit error rate (BER) of less than 10^{-9}. The system's maximum range was 1200 m for Alexandria and 1100 m for Chandigarh. The proposed model can be suggested for use in next generation (NG) passive optical networks (PON) for supporting symmetric 40 Gb/s data.

Introduction

Currently, the proliferation of data centers and the emergence of new applications such as cloud computing architectures, Internet of Things (IoT), and online games and movies on smartphones have spurred the development of new technologies to enhance the capacity of optical fiber cable (OFC) network and optimize the optical spectrum [1–3]. Different multiplexing techniques that uses time slots like time division multiplexing (TDM) for sending information on them [4,5], or different frequencies like frequency division multiplexing (FDM) [6], and wavelength division multiplexing (WDM) are used in the OFC network for capacity enhancement [7–10]. Despite the use of both time and WDM techniques together such as TWDM in PON, their existence is costly from the perspective of an Internet service provider (ISP), and they rely on existing legacy gigabit networks like the gigabit passive optical network (GPON), 10 gigabits passive optical network (10GPON), 10 gigabit Ethernet passive optical network (10GE-PON), and 10 gigabits symmetrical passive optical network (XGS-PON) infrastructures. As a result, a coexistence access network with symmetric 1.25, 2.5, and 10 Gbps channels is being developed [11] where these PONs use SMF.

However, a large amount of information data still remains to be transmitted via these multiplexing techniques regarding meeting the needs of the end users [12,13]. The demand for using multimode fiber (MMFs) has become essential due to its ability to provide a high

* Corresponding author.
E-mail addresses: syedalwee@unimap.edu.my (S. Alwee Aljunid), h.ahmed@psau.edu.sa (H. Yousif Ahmed), m.zeghid@psau.edu.sa (M. Zeghid), n.sooppy@psau.edu.sa (K.S. Nisar).

https://doi.org/10.1016/j.rinp.2023.106656
Received 7 May 2023; Received in revised form 5 June 2023; Accepted 16 June 2023
Available online 17 June 2023

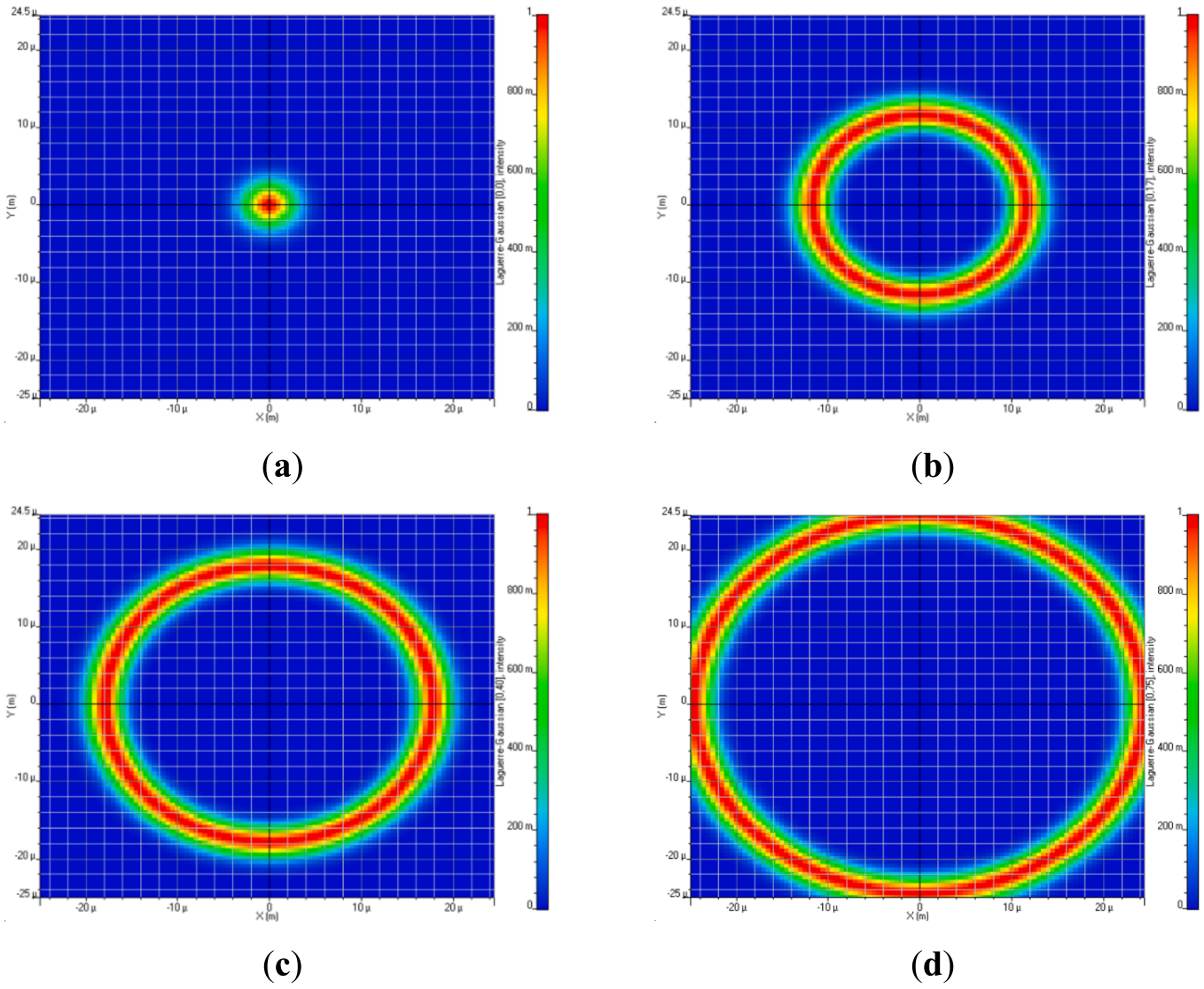

Fig. 1. Intensity profiles for different OAM modes. (**a**) $LG_{0,0}$ ($h = 0$, $m = 0$); (**b**) $LG_{0,17}$ ($h = 0$, $p = 17$); (**c**) $LG_{0,40}$ ($h = 0$, $m = 40$); (**d**) $LG_{0,75}$ ($h = 0$, $m = 75$).

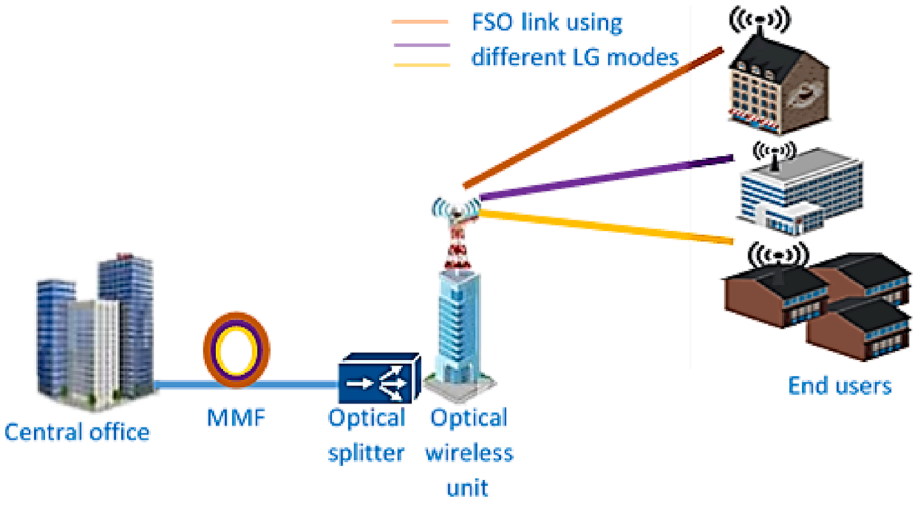

Fig. 2. Layout of the hybrid MMF/FSO system.

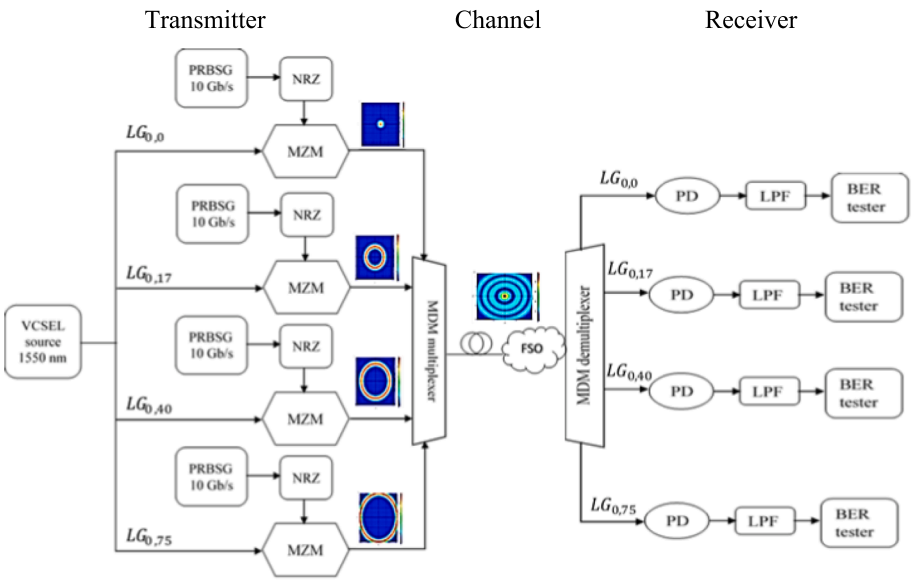

Fig. 3. Block diagram of the proposed MMF/FSO system based on the OAM beams.

Table 1
Simulation parameters [31,41,49].

Parameter	Type or value
Data generator	
Data rate per channel	10 Gbps
Electrical generator	
Modulation type	NRZ
Modulation rectangular shape	Exponential
Electrical bandwidth	0.75 × bit rate Hz
Optical source	
Centered wavelength	1550 nm
VCSEL input power	15 dBm
Linewidth of VCSEL	10 MHz
OAM modes	$LG_{0,0}$, $LG_{0,13}$, $LG_{0,40}$, and $LG_{0,80}$
MMF parameters	
Length	100 m
Attenuation	2.61 dB/km
FSO channel	
Beam divergence	2 mrad
Transmitter aperture diameter	10 cm
Weather conditions considered	CW, various rainfall, and fog
Attenuation of CW	0.14 dB/km
Atmospheric turbulences considered	WT and ST
Turbulence model	Gamma–Gamma distribution
Receiver aperture diameter	20 cm
Photodetector	
Responsivity	1 A/W
Receiver load resistance	1030 Ω
Thermal noise power density	10^{-22} W/Hz
Receiver noise temperature	300 K

bandwidth, and the existing transmission technology that depends on using single mode fiber (SMF) is about to reach the capacity limits [14,15]. Additionally, for further capacity enhancement, OFC networks are used with optical wireless communications (OWC) such as free space optics (FSO). The FSO communication system has many advantages such as high security, high speed transmission, no interference with electromagnetic waves, and a license-free spectrum [16–19], which makes its use with OFC capable of providing these services to end users [20,21]. A recent technology, which is mode division multiplexing (MDM), is used to enable high speed data transmission in optical communication networks [22]. In MDM, the information data signals are transmitted either through a specific mode or group modes in OFC [22]. orbital angular momentum (OAM) modes are preferred to be used in hybrid MMF/FSO transmission systems among other orthogonal modes used in MDM [23]. The modes exhibit doughnut ring-shaped intensity patterns and helical phases that rotate orthogonally during propagation [24]. Laguerre-Gaussian (LG) modes are utilized for 2D modal analysis in OAM modes [25–27]. In order to facilitate the initiation of OAM modes and ensure alignment with optical connections, microscale spiral-phased plates have been directly inserted into the aperture of a vertical-cavity surface-emitting laser (VCSEL) [28]. The low power consumption and cost-effectiveness of the VCSEL have earned it a place in the data center industry [29]. Recently, there have been several studies by researchers who used hybrid OFC with FSO systems for capacity enhancement. In [2], a MDM based on using four LG modes was integrated into the hybrid SMF/FSO system, and the simulated results reported that an overall capacity of 40 Gb/s was transmitted along 10,950 m (10,000 m SMF length + 950 m FSO range). In [29], a hybrid SMF/FSO was proposed based on using orthogonal FDM, polarization division multiplexing (PDM), and a reflective semiconductor optical amplifier (SOA). A total transmission distance of 50,008 m (50,000 m SMF length + 8 m FSO range) with a transmission capacity of 10 Gb/s in the uplink and 5 Gb/s in the downlink is achieved. In [30], different levels of quadrature amplitude modulation (QAM) were used in a hybrid SMF/FSO system and a transmission capacity of 34, 67, and 100 Mbps were achieved, respectively, when 4-QAM, 16-QAM, and 64-QAM signals were used, respectively. Additionally, a total transmission distance of 10,002 m (10,000 m SMF length + 2 m FSO range) was achieved. A hybrid MMF/FSO based on using two spiral phase donut modes was proposed in [31]. The results reported a transmission of 80 Gb/s for a distance of 2170 m (100 m MMF length + 2070 m FSO range).

The main objectives of this work, based on recent published studies, are as follows:

a. Introducing a new hybrid MMF/FSO based on using the MDM of four independent OAM beams ($LG_{0,0}$, $LG_{0,17}$, $LG_{0,40}$, and $LG_{0,75}$) for capacity enhancement to be used in data centers and 5G passive optical networks.

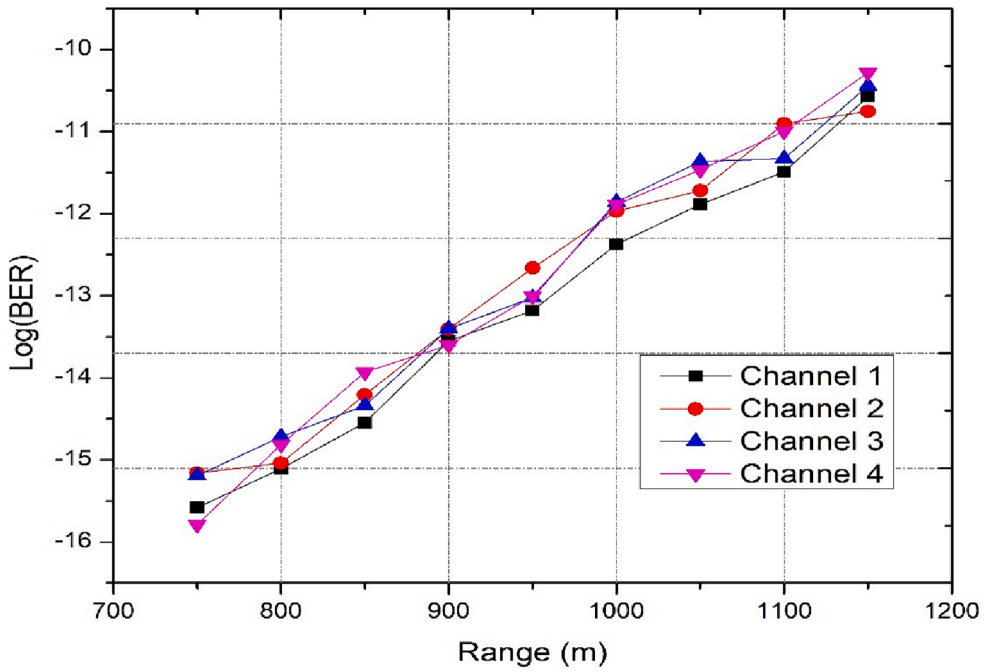

Fig. 4. The log(BER) for the proposed hybrid MMF/FSO model using four OAM beams under the CW versus FSO propagation range.

b. While the proposed hybrid MMF/FSO system can used in different broadband services, the attenuation caused by external climate changes such as clear, rain and fog, and turbulence have a negative impact on the received signal. Therefore, studying their effects was considered in this work.
c. Using the real meteorological data of different cities located in different countries and continents are considered to learn the availability of implementing our proposed model in a real environment.

In this paper, we proposed a hybrid MMF/FSO system based on using MDM for use as a solution for providing services to end users located in remote areas. Four OAM beams ($LG_{0,0}$, $LG_{0,17}$, $LG_{0,40}$, and $LG_{0,75}$) are used, each carrying 10 Gb/s, resulting in an overall capacity of 40 Gb/s. A fixed length of 100 m was used for the MMF cable while various FSO ranges were used according to the weather condition or turbulence effect. The information signal is first travelled a 100 m in MMF channel then propagates in FSO channel. Transmission ranges and BER were used as performance metrics for investigating the models' performance. Clear weather (CW), various levels of rainfall (light rainfall (LR), medium rainfall (MR), and heavy rainfall (HR)), and different degrees of fog (light fog (LF), medium fog (MF), and heavy fog (HF)) were the weather conditions considered. Additionally, the performance of the proposed hybrid MMF/FSO based on real meteorological data from the cities of Alexandria and Chandigarh for the years 2014–2018 was investigated.

The rest of this paper is organized as follows. A description for the OAM modes is given in Sec. 2 while the structure of the proposed hybrid MMF/FSO system based on using OAM beams is given in Sec. 3. The proposed model's performance analysis based on its transmission in the FSO channel is presented in Sec. 4. The simulation results and discussion are provided in Sec. 5. The conclusions drawn from the study are presented in Sec. 6.

Orbital angular momentum (OAM) modes

Light waves, when propagating, can use OAM beams to carry the information data without performing any signal processing. The distinguishing between various OAM beams is based on their helical phase front. The light waves that carry the OAM beam are characterized by a spiral phase structure that is represented as $e^{ih[03B8]}$, where h and θ are the number of 2 π phase shifts and the azimuthal angle, respectively [32–34]. Theoretically, OAM beams have an infinite number of h, leading to an unlimited number of states. These states are orthogonal and propagate coaxially with each other [35]. Unfortunately, in practical FSO connections, the number of h is limited as it is restricted by the size of the receiver telescope (the OAM beam waist, w_0, increases proportionally to $\sqrt{h}$) [24].

Practically, there are three methods are available for generating OAM beams using diffractive optics, which are spiral phase plates, computed-generated holograms, and diffractive optical elements [36]. Additionally, there are several methods that can be used to detect the OAM beams like Fresnel bi prisms, wedged optical flats, diffraction patterns of triangular apertures, and tilted converging spherical lenses or cylindrical [37].

LG modes are used with OAM beams for 2D modal analysis, which are solutions to the paraxial wave equation [27]. The two indices that must be found in each *LG* mode are h, which is used for azimuthal distribution, and m, which is used for radial distribution [27].

For any two OAM beams, the orthogonality between them is given as [38]

$$\int_0^{2\pi} u_1(\rho,[03B8],z)u_2^{*}(\rho,[03B8],z)d\theta = \int_0^{2\pi} A_1(\rho,z)e^{ih_1\theta}A_2^{*}(\rho,z)e^{-ih_2\theta}d\theta = \begin{cases} 0 if h_1 \neq h_2 \\ A_1A_2^{*} if h_1 = h_2 \end{cases} \quad (1)$$

where $(\rho,[03B8],z)$ is the cylindrical coordinate while ρ, z, and θ refer to the radial direction, the direction of propagation along the z-axis coordinate, and angular direction, respectively.

The electric field of the *LG*, $E(\rho,[03B8],z;h,m)$ is expressed as [39]

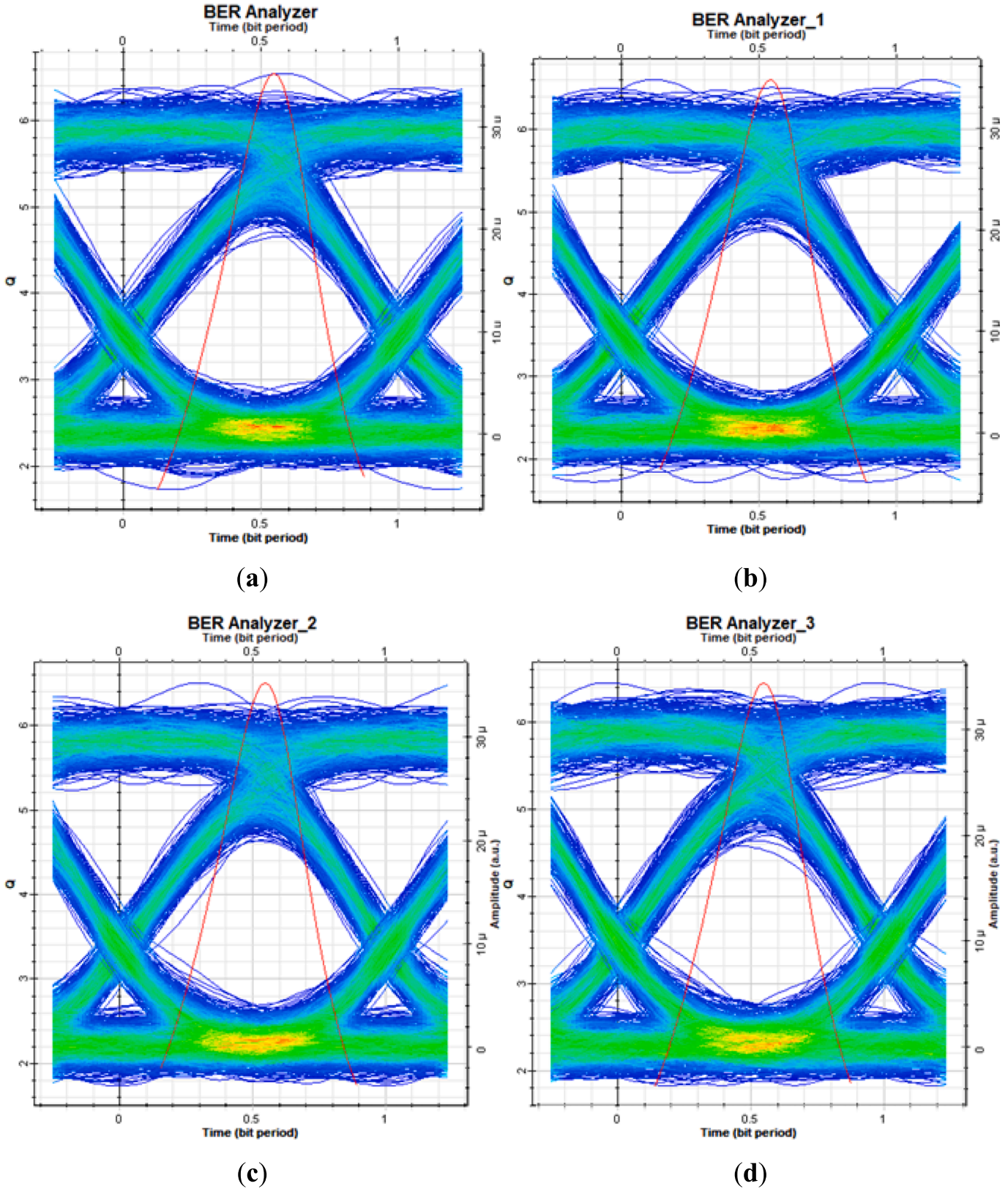

Fig. 5. Eye diagrams for the four channels of the proposed hybrid MMF/FSO system after a 100 m MMF length and 1150 m FSO range (**a**) $LG_{0,0}$; (**b**) $LG_{0,17}$; (**c**) $LG_{0,40}$; (**d**) $LG_{0,75}$.

Table 2
The log(BER) corresponding to 1250 m under CW.

Channel	*LG* Beam	Log(BER)
1	$LG_{0,0}$	−10.57
2	$LG_{0,17}$	−10.75
3	$LG_{0,40}$	−10.44
4	$LG_{0,75}$	−10.28

$$E(\rho,[03B8],z;h,m)=\sqrt{\frac{2m!}{\pi(m+|h|)!}}\frac{1}{\omega(z)}\left[\frac{\rho\sqrt{2}}{\omega(z)}\right]^{|h|}L_{h,m}\left[\frac{2\rho^2}{\omega^2(z)}\right]\times exp\left[\frac{-\rho^2}{\omega^2(z)}\right]exp\left[\frac{-ic\rho^2 z}{2(z^2+z_R^2)}\right]\times exp\left[i(2m+|h|+1)tan^{-1}\frac{z}{z_R}\right]\exp(-ih\theta) \quad (2)$$

where $\omega(z)$ is the beam waist size at z distance; c is the optical wave number and is equal to $(2\,\pi/\lambda)$; z_R is the Rayleigh range; and $L_{h,m}$ is the *LG* polynomial.

Fig. 1 displays the *LG* modes' intensity profiles which were used in this work ($LG_{0,0}$, $LG_{0,17}$, $LG_{0,40}$, and $LG_{0,75}$).

Proposed hybrid MMF/FSO system based on using OAM beams

The layout of the hybrid MMF/FSO system based on using different *LG* beams is shown in Fig. 2. It consists of a central office that is responsible for transforming the internal backbone network traffic into optical wavelengths as well as delivering data signals through using a hybrid MMF cable and FSO channels to the user premises.

The block diagram of the proposed MMF/FSO based on using four OAM beams is given in Fig. 3. It consists of three main parts, which are the transmitter, channel (two channels were used, MMF and FSO), and receiver. The transmitter consists of four components: the data generator, electrical generator, laser source, and Mach–Zehnder modulator (MDM) and that are presented in central office. The data generator is a pseudo random bit sequence generator (PRBSG) and is responsible for generating 10 Gb/s information data, which are then entered into the electrical generator. The type of electrical generator is a non-return-to-zero (NRZ) on–off keying. The VCSEL source is used for generating the *LG* beams ($LG_{0,0}$, $LG_{0,17}$, $LG_{0,40}$, and $LG_{0,75}$). Afterwards, the electrical signals are modulated onto the optical signals using the MZM. The optical signals from the 4 *LG* beams are then multiplexed by MDM multiplexer before travelling to the channel. Two channels are used, which are MMF and FSO. The signal is first transferred in an MMF with a fixed length of 100 m and then propagated in the FSO channel with various propagation ranges according to the weather conditions and atmospheric turbulence. Then, the signal is received at the receiver while an MDM demultiplexer is used for separating the received signals from the different *LG* modes. Each receiver has a photodetector (PD) to detect the required channel and the output electrical signal from the PD is filtered by a low pass filter (LPF), which further goes through the BER analyzer to show the performance of the received data.

Mathematical model of proposed MMF/FSO transmission system

The current reached at the PD is given by [40]:

$$I_{PD}=P_r B_o \Re \quad (3)$$

where B_o is the optical bandwidth; $\Re$ is the responsivity of the PD; and P_r is the received power. The P_r can be expressed in terms of the transmitted power, P_t; atmospheric attenuation, $\propto_{atm}$; FSO propagation range, L; beam divergence angle, $\varnothing$; transmitter aperture diameter, d_t; and receiver aperture diameter, d_r, as [41]

$$P_r=P_t\left(\frac{d_r}{d_t+\varnothing L}\right)^2 10^{\frac{-\propto_{atm}L}{10}} \quad (4)$$

As the rain and fog weather conditions were considered in this work, the atmospheric attenuation caused by them can be expressed as [42]

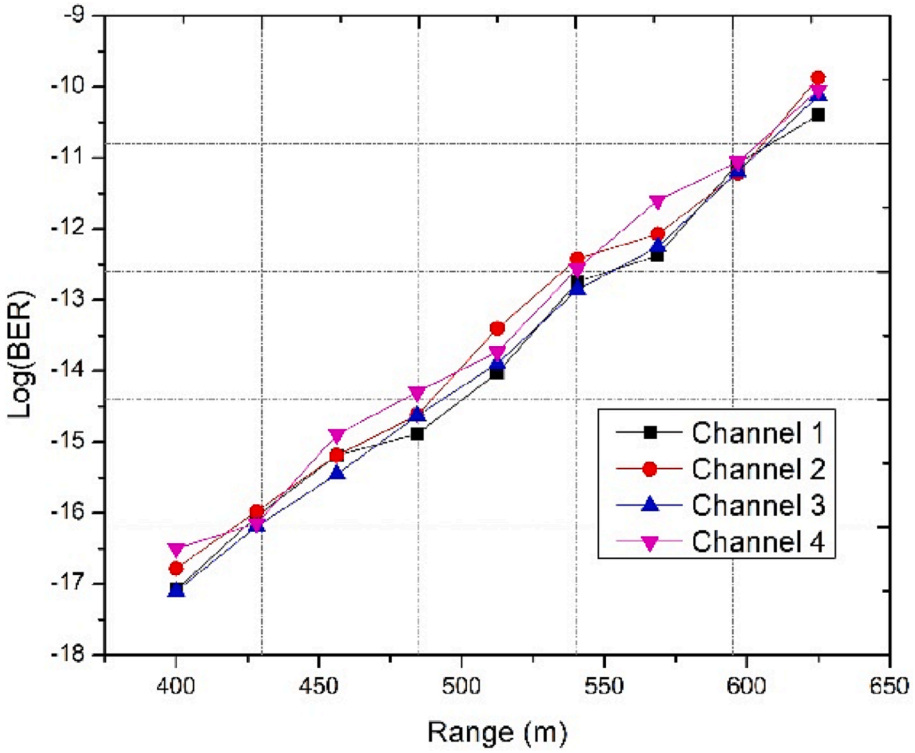

Fig. 6. Log(BER) Vs FSO span under LR for the proposed hybrid MMF/FSO model.

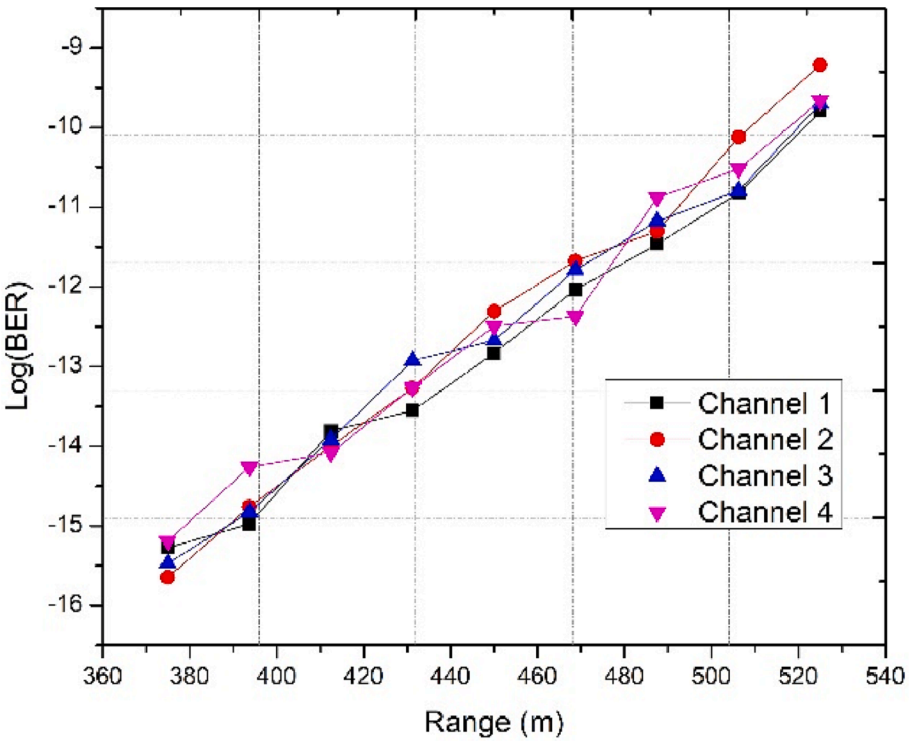

Fig. 7. Log(BER) Vs FSO span under MR for the proposed hybrid MMF/FSO model.

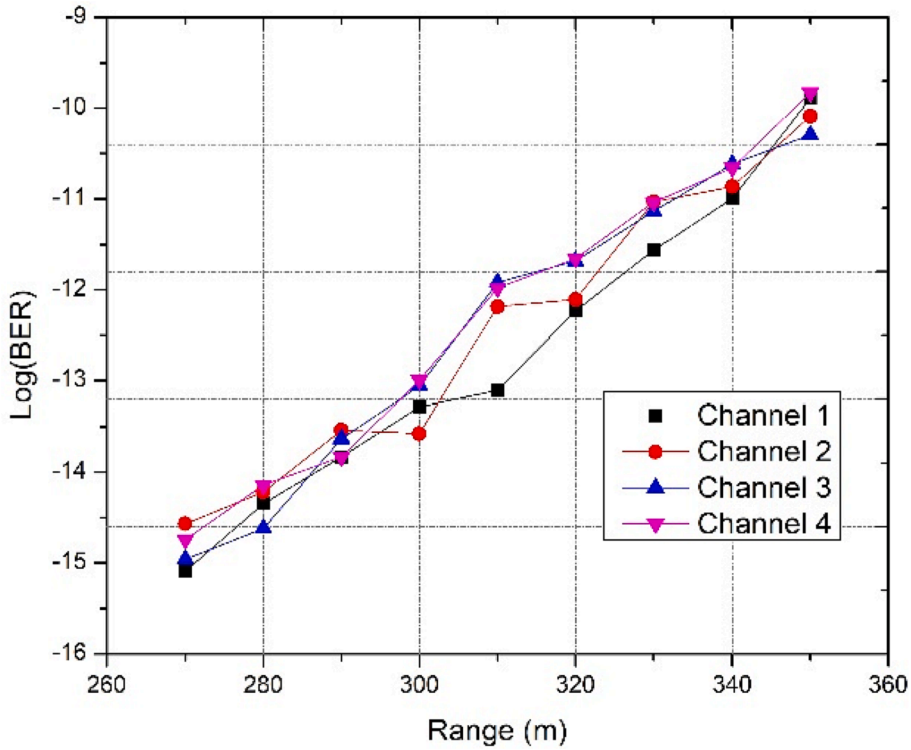

Fig. 8. Log(BER) Vs FSO span under HR for the proposed hybrid MMF/FSO model.

$$\alpha_{atm-rain} = 1.07R^{0.67} \tag{5}$$

$$\alpha_{atm-fog} = \frac{3.912}{V}\left(\frac{\lambda}{550nm}\right)^{-s} \tag{6}$$

where R refers to the rate of the rainfall and is equal to 7.22×10^{-4} cm/s for LR, 1.11×10^{-3} cm/s for MR, and 2.22×10^{-3} cm/s for HR [43]; V refers to the visibility range; and s is the size distribution of the scattering particle and its value differs according to the value of V, which is equal, according to the Kim model, to 1.6 if V greater than 60, 1.3 if V greater than 6 but less than 50, 0.16 $V + 0.34$ if V greater than 1 but less than 6, $V - 0.5$ if 0 V greater than 0.5 but less than 6, and 0 if V less than

Table 3
The log(BER) corresponding to 725 m under LR, 625 m under MR, and 450 m under HR.

Channel	*LG* Beam	Rain Condition	Log(BER)
1	$LG_{0,0}$	LR	−10.39
		MR	−9.78
		HR	−9.89
2	$LG_{0,17}$	LR	−9.86
		MR	−9.21
		HR	−10.08
3	$LG_{0,40}$	LR	−10.12
		MR	−9.69
		HR	−10.29
4	$LG_{0,75}$	LR	−10.04
		MR	−9.66
		HR	−9.83

0 [44,45].

Atmospheric turbulence also has an effect on the optical signal during its transmission in the FSO channel due to variations in temperature. The refractive index structure, C_n^2, of the transmission channel (air) fluctuates from $5 \times 10^{-16}\,\mathrm{m}^{\frac{-2}{3}}$ for weak turbulence (WT) to $5 \times 10^{-14}\mathrm{m}^{\frac{-2}{3}}$ for strong turbulence (ST). There are several models such as log-normal (which characterizes the WT and is suitable for FSO communication under CW) [43], K-distribution (which suitable for ST) [46], and gamma–gamma, which is widely used and applicable for different turbulences of either WT or ST [47]. The gamma–gamma model was considered in this paper, in which the irradiance/intensity of the normalized light is defined by the large eddy scale,α, and small eddy scale, β, which follow a gamma distribution, leading to a gamma–gamma distribution with a probability density function (PDF) of [48,49]

$$PDF = \frac{2(\propto\beta)^{\frac{\alpha+\beta}{2}}}{\Gamma(\alpha)\Gamma(\beta)} I_s^{\frac{(\alpha+\beta)}{2}} K_{\alpha-\beta}\left(2\sqrt{\alpha\beta h_s}\right); h_s > 0 \tag{7}$$

$$\alpha = \left[\frac{0.51\sigma_r^2}{\left(1+0.69\sigma_r^{\frac{12}{5}}\right)^{\frac{5}{6}}}\right] - 1 \tag{8}$$

$$\beta = \left[\frac{0.49\sigma_r^2}{\left(1+1.11\sigma_r^{\frac{12}{5}}\right)^{\frac{5}{6}}}\right] - 1 \tag{9}$$

where $K_i()$ indicates the i th order of the modified Bessel function; $\Gamma()$ refers to the Gamma function; and σ_r^2 is the Rytov variance, which depends on C_n^2.

The shot noise, *SN*, and thermal noise, *TN*, are expressed as [40,44]:

$$SN = 2eB_e\Re\langle I_{PD}\rangle \tag{10}$$

$$TN = \frac{4k_BTB_e}{R_L} \tag{11}$$

where e, k_B, R_L, B_e, and T, are the electron charge, Boltzmann constant, receiver load resistance, electrical bandwidth, and absolute temperature of the receiver, respectively.

The *SNR* is then expressed as [24,48]

$$SNR = \frac{(I_{PD})^2}{SN + TN} \tag{12}$$

Finally, the BER is given in terms of *SNR* as [48]

$$BER = \frac{1}{2} erfc\left(\frac{\sqrt{SNR}}{2\sqrt{2}}\right) \tag{13}$$

where *erfc* is the error complementary function.

Results and discussion

The proposed hybrid MMF/FSO using four OAM beams was simulated using Optisystem Software ver. 19 with the parameters given in

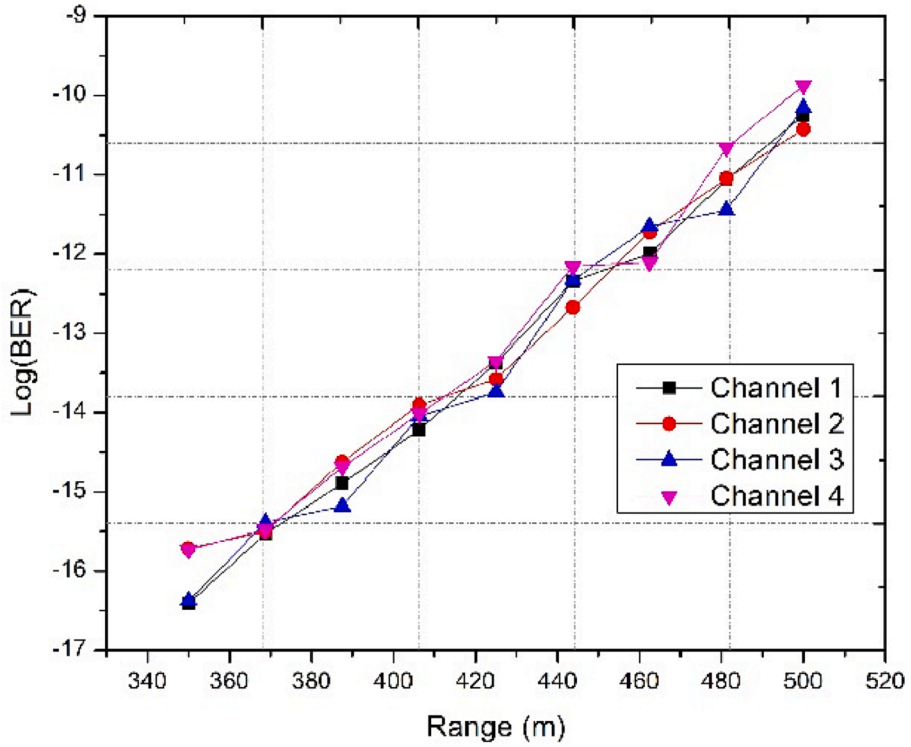

Fig. 9. Log(BER) Vs FSO span under LF for the proposed hybrid MMF/FSO model.

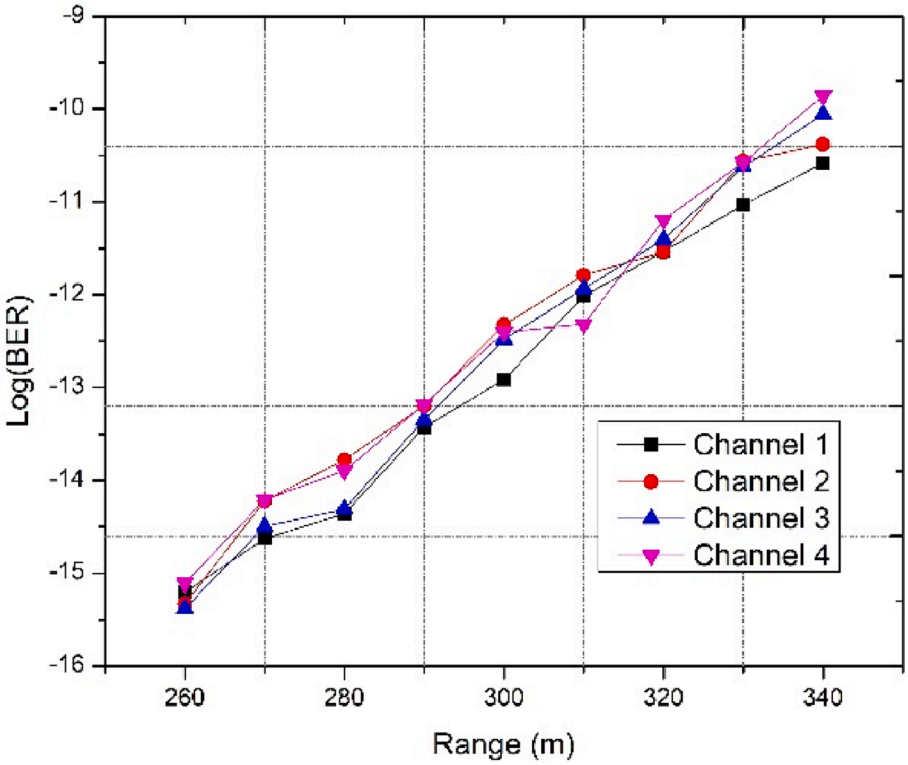

Fig. 10. Log(BER) Vs FSO span under MF for the proposed hybrid MMF/FSO model.

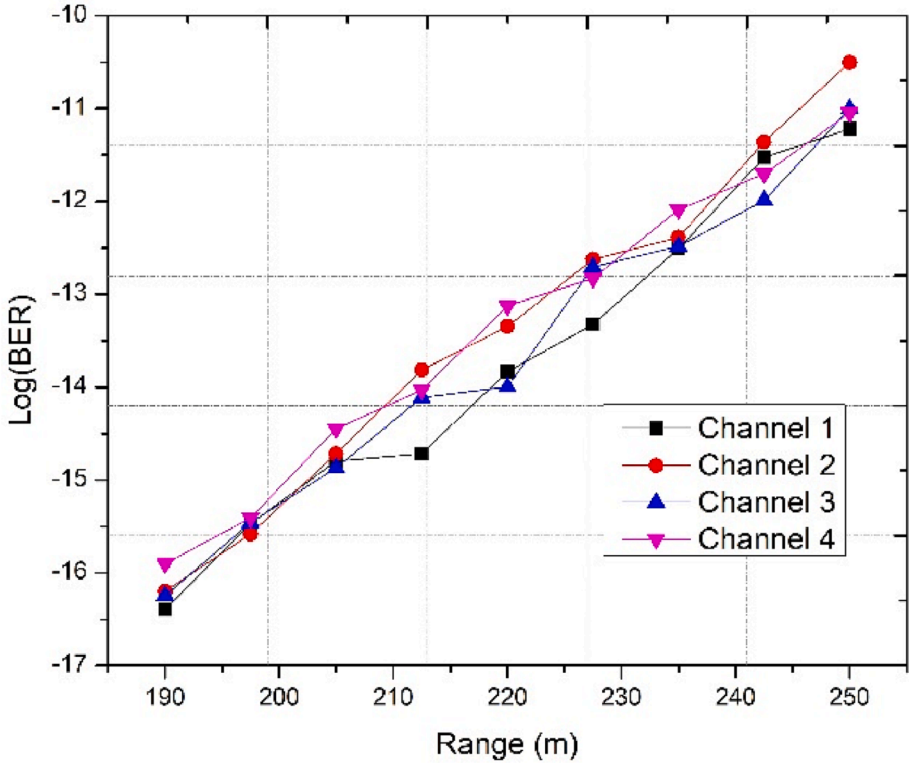

Fig. 11. Log(BER) Vs FSO span under HF for the proposed hybrid MMF/FSO model.

Table 1 [31,41,49]. Performance was investigated in terms of the maximum achievable range and BER. The findings are exhibited in five parts. The first part shows the results for the performance of the proposed model when propagated under CW, while the second and third parts show the effects of the different rain and fog conditions, respectively. The effects of turbulence are discussed in the fourth section, followed by the effects of weather conditions in Alexandria, Egypt, and Chandigarh, India. Additionally, in this section, a fixed length of 100 m

Table 4
Log(BER) values for the four channels under LF, MF, and HF correspond to 600 m, 440 m, and 350 m overall transmission ranges, respectively.

Channel	*LG* Beam	Rain Condition	Log(BER)
1	$LG_{0,0}$	LF	−10.24
		MF	−10.58
		HF	−11.21
2	$LG_{0,17}$	LF	−10.42
		MF	−10.37
		HF	−10.50
3	$LG_{0,40}$	LF	−10.15
		MF	−10.05
		HF	−11
4	$LG_{0,75}$	LF	−9.87
		MF	−9.85
		HF	−11.04

for MMF and various FSO ranges according to the external climate weather are considered.

Clear weather

The log(BER) performance for the hybrid MMF/FSO system using four OAM beams when propagating under CW weather is given in Fig. 4. It is clear from Fig. 4 that as the proposed model traveled a long FSO range, the log(BER) increased, leading to a degradation in the performance of the hybrid MMF/FSO system. At an FSO range of 1150 m, the log(BER) of the four channels ($LG_{0,0}$, $LG_{0,17}$, $LG_{0,40}$, and $LG_{0,75}$ was <-10, indicating that all of the transmitted information data (40 Gb/s) were successfully received as the threshold value of BER is $<10^{-9}$.

The eye diagrams for the four channels that were transmitted using $LG_{0,0}$, $LG_{0,17}$, $LG_{0,40}$, and $LG_{0,75}$ beams after a 100 m MMF length and 1150 m FSO range are displayed in Fig. 5. The wider eye opening showed the successful reception of the transmitted data for all channels.

Table 2 shows the log(BER) values corresponding to 1250 m (100 m MMF + 1150 m FSO range) for the four channels under CW.

Various rainfall (LR, MR, and HR)

In this part, the impact of various rainfall rates on the performance of the hybrid MMF/FSO system is discussed. Rain causes a different attenuation, which varies from 6.27 dB/km (LR) to 19.28 dB/km (HR) according to the rainfall intensity and amount. Additionally, for the average amount of rainfall, the attenuation is 9.64 dB/km [41]. Figs. 6–8 show the log(BER) versus different propagation ranges for the proposed hybrid MMF/FSO system under LR, MR, and HR. It can be observed from Figs. 6–8 that longer ranges and heavier rainfall intensities caused higher log(BER) values, while lower log(BER) values were achieved for the low rainfall intensities and the short FSO propagation ranges. As an example of channel 1, which uses the $LG_{0,0}$ beam under the HR condition, the log(BER) was −13.10 at a 310 m FSO range, which increased to −9.89 when the proposed hybrid model travelled a 40 m longer propagation range.

Table 3 shows the values of the log(BERs) for the four channels corresponding to 725 m (100 m MMF + 625 m FSO range) under LR, 625 m (100 m MMF + 525 m FSO range) under MR, and 450 m (100 m MMF + 350 m FSO range) under HR.

Foggy weather

The influence of different degrees of fog on the hybrid MMF/FSO system's performance will be investigated in this section. Fog is caused when smoke is floating in the air. As the degree of fog increases, the visibility decreases and the attenuation increases, leading to a degradation in the received information signal. When the level of the fog is at its heaviest, the attenuation caused by it is 30 dB/km, which decreases to 20 dB/km when the level of fog is moderate. It also drops to a low of 10 dB/km when there is light fog. Fig. 9 depicts the performance of the suggested hybrid MMF/FSO model when propagating under the effect of

Table 5
The log(BER) corresponding to 1250 m under WT and ST.

Channel	*LG* Beam	Log(BER)	
		WT	ST
1	$LG_{0,0}$	−9.07	−4.86
2	$LG_{0,17}$	−9.18	−5.02
3	$LG_{0,40}$	−9.48	−4.77
4	$LG_{0,75}$	−9.12	−4.81

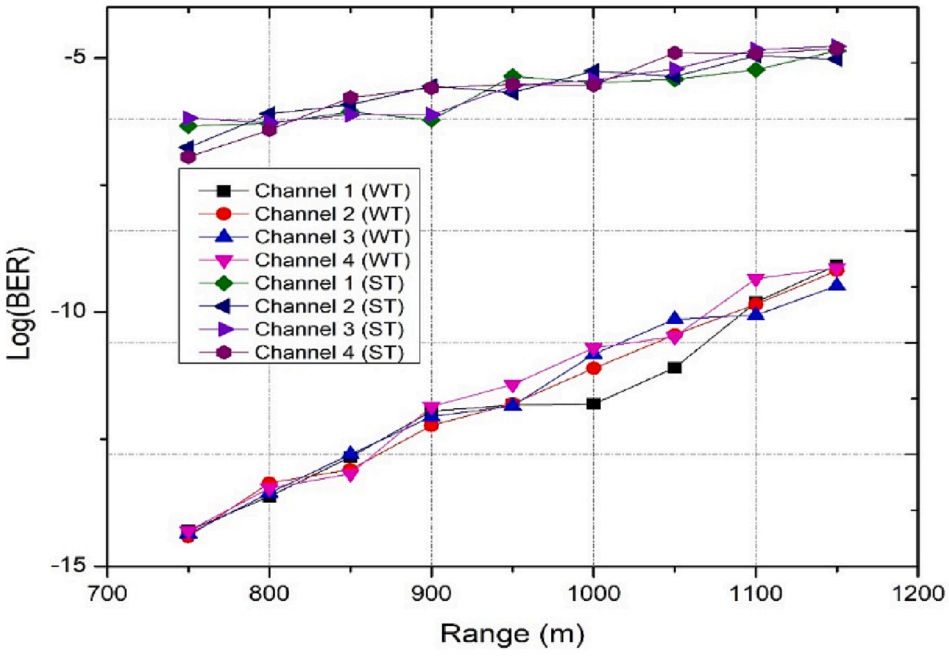

Fig. 12. The log(BER) under WT and ST for the proposed hybrid MMF/FSO model versus the FSO range.

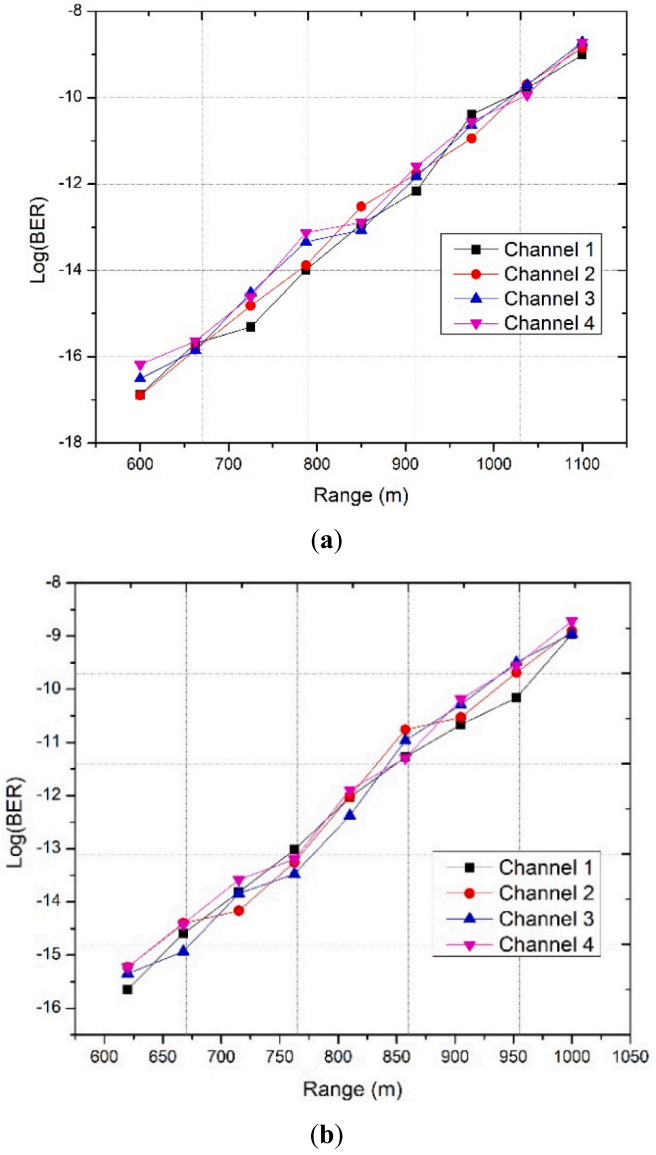

Fig. 13. The log(BER) for the hybrid MMF/FSO model versus the FSO range under the weather of (**a**) Alexandria and (**b**) Chandigarh.

Table 6
The log(BER) corresponding to 1200 m for Alexandria and 1000 m for Chandigarh.

Channel	*LG* Beam	Log(BER)	
		Alexandria	Chandigarh
1	$LG_{0,0}$	−9.01	−8.96
2	$LG_{0,17}$	−8.84	−8.90
3	$LG_{0,40}$	−8.71	−8.95
4	$LG_{0,75}$	−8.72	−8.71

LF. As the ranges varied from 350 m to 500 m, the log(BER) values increased from −16 to −10 for all four channels using different OAM beams. Similarly, in Figs. 10 and 11, which show the results of log(BER) versus the variation in the FSO ranges under MF and HF, the performance degraded as the transmission distances increased. When the ranges that channel 1 could travel under LF, MF, and HF were compared, it was discovered that the longest range was achieved under an LF at 500 m, which decreased to 340 m and 250 m under MF and LF, respectively. These values were obtained for a log(BER) value < -9.

Table 7
Comparison between the present work and previous published works.

Ref.	[30]	[31]	Present Work
Technique	PDM/OFDM	Different levels of QAM	MDM
Channel	SMF + FSO	SMF + FSO	MMF + FSO
External climate conditions	Not considered	Not considered	CW, LF, MF, HF, LR, MR, and HR
Atmospheric turbulences	Not considered	Not considered	WT and ST
Real meteorological data	Not considered	Not considered	Alexandria in Egypt and Chandigarh in India
Overall capacity	10 Gb/S	100 Mbps	40 Gb/s

Additionally, when comparing the results of the proposed model under fog conditions with those under the rain conditions, it was observed that the ranges achieved under various rainfall rates were longer than those achieved under fog conditions, which was expected as fog causes a greater attenuation value than rain.

The log(BER) values for the four channels corresponding to 600 m (100 m MMF + 50 m FSO range) under LF, 440 m (100 m MMF + 340 m FSO range) under MF, and 350 m (100 m MMF + 250 m FSO range) under HF are summarized in Table 4.

Effect of different turbulence conditions

The atmospheric turbulence impacted the propagation of the information signal through the FSO channel. Accordingly, in this part, the results of different turbulences (WT and ST) on the performance of the proposed hybrid MMF/FSO system are evaluated. Fig. 12 depicts the log (BER) of the proposed model under the effect of WT and ST against the different transmission ranges. It is clear that for low WT ($C_n^2 = 5 \times 10^{-16} m^{\frac{-2}{3}}$), all the channels using the hybrid MMF/FSO system could propagate up to 1150 m with a log(BER) of approximately −9. Therefore, the information data could be received successfully at the receiver. However, when ST ($C_n^2 = 5 \times 10^{-14} m^{\frac{-2}{3}}$), the performance of the received signal degraded. At the same range (1150 m), it can be observed from Fig. 12 that the value of the log(BER) increased to −4.7.

Table 5 tabulates the values of the log(BER) for the four channels corresponding to 1250 m (100 m MMF + 1150 m FSO range) under the effect of WT and ST.

Performance of proposed hybrid MMF/FSO model for Alexandria and Chandigarh cities

As it is important to show the applicability of implementing the proposed hybrid MMF/FSO system in a real environment, we considered all of the parameters used in the simulation according to those used in practical systems. Additionally, the real meteorological data for the years 2014–2020 for the two cities, Alexandria and Chandigarh, were considered. Regarding Alexandria, the data were collected from https://www.worldweatheronline.com (accessed on 25 February 2023), which shows that the average visibility range was 9.8 km, which according to Eq. (6), caused an attenuation of 0.1 dB/km. Regarding Chandigarh, the attenuation was 1.9 dB/km [42]. The relation between the log(BER) values and the various FSO ranges for the proposed MMF/FSO system under the weather of these two cities is given in Fig. 13. The coastal area where Alexandria is located allows the information signals carried by the four channels to travel a longer distance than that achieved by Chandigarh. At log(BER) 10^{-9}, the proposed model achieved an FSO link of 1100 m for Alexandria, which decreased to 1000 m for Chandigarh, which was expected, as attenuation caused by the weather in Alexandria is lower than that caused by the weather in Chandigarh.

Table 6 shows the values of the log(BER) for the four channels corresponding to 1200 m (100 m MMF + 1100 m FSO range) and 1100 m (100 m MMF + 1000 m FSO) for Alexandria and Chandigarh,

respectively.

Table 7 provides a comparison between our study and previous publications.

Conclusions

The importance of having high-speed transmission systems with high capacity has become urgent nowadays due to the increase in data traffic, so in this paper, a new hybrid MMF/FSO system based on OAM multiplexing was proposed. A single wavelength was used to carry four distinct LG beams ($LG_{0,0}$, $LG_{0,17}$, $LG_{0,40}$, and $LG_{0,75}$), each carrying 10 Gb/s data, resulting in a $4\times10 = 40$ Gb/s overall capacity. Two propagation channels were used, the first channel was the MMF cable with a fixed length of 100 m, and the second channel was the FSO channel. As in the FSO channel, the signal propagated in the atmosphere, so it was exposed to different climate changes and different atmospheric turbulences. Accordingly, CW, various rainfall rates, and different degrees of fog conditions were considered in evaluating the performance of the hybrid MMF/FSO system. Additionally, the impact of different turbulences either weak or strong on the proposed model's performance was investigated. To implement the proposed model in a real environment, the real data of the weather of two different cities, Alexandria and Chandigarh, were considered, and the performance was also studied under their effects. The simulation results revealed that the proposed model could successfully travel a 100 m MMF in addition to different FSO ranges that varied from 1150 m under the effect of CW to 250 m under the effect of HF with a log(BER) less than or equal to -9. Furthermore, the transmission distance of the proposed model used in Alexandria was 1200 m (100 m MMF + 1100 m FSO link), which needs to be decreased to 1000 m (100 m MMF + 1000 m FSO link) if used in Chandigarh. Consequently, as our model can enhance capacity and support high speed data transmission, so we recommended to be implemented in 5G PONs, remote areas, urban areas, and future hybrid MMF/FSO data center interconnects. For future works, we suggest other multiplexing techniques such as polarization division multiplexing, and orthogonal FDM with our proposed model for further capacity enhancement. We also need to demonstrate our model experimentally in order to consider the real-time losses and inter modal cross talk.

CRediT authorship contribution statement

Mehtab Singh: Writing – original draft, Methodology, Conceptualization. **Somia A. Abd El-Mottaleb:** Writing – original draft, Software, Methodology, Formal analysis. **Syed Alwee Aljunid:** Validation, Writing – original draft. **Hassan Yousif Ahmed:** Writing – review & editing, Writing – original draft, Software, Investigation. **Medien Zeghid:** Validation, Writing – original draft, Investigation. **Kottakkaran Sooppy Nisar:** Investigation, Software, Validation, Writing - original draft, Writing - review & editing.

Declaration of Competing Interest

The authors declare that they have no known competing financial interests or personal relationships that could have appeared to influence the work reported in this paper.

Data availability

No data was used for the research described in the article.

Acknowledgement

This study is supported via funding from Prince Sattam bin Abdulaziz University project number (PSAU/2023/R/1444).

References

[1] Sarmiento S, Spadaro S, Lazaro JA. Cost-effective ROADM design to maximize the traffic load capacity of u-DWDM coherent metro-access networks. Opt Switch Netw 2018;30:53–61.
[2] Singh, H.; Mittal, N.; Miglani, R.; Majumdar, A.K. Mode division multiplexing (mdm) based hybrid PON-FSO system for last-mile connectivity. In Proceedings of the 2021 Third South American Colloquium on Visible Light Communications (SACVLC), Toledo, Brazil, 11–12 November 2021.
[3] Pile, D. Compact multiplexing. *Nat. Photon* **2015**, *9*, 78.
[4] Harstead E, Van Veen D, Houtsma V, Dom P. Technology roadmap for time-division multiplexed passive optical networks (TDM PONs). J Light Technol 2019;37:657–94.
[5] Dong T, Shen G. Traffic grooming for IP over WDM optical satellite networks November 2014;9–10:1–6.
[6] Armstrong J. OFDM for optical communications. J Light Technol 2009;27:189–204.
[7] Singh M, Aly MH, El-Mottaleb SAA. Performance analysis of a 448 Gbps PDM/WDM/16-QAM hybrid SMF/FSO system for last mile connectivity. Opt Quant Electron 2023;55:231.
[8] Cikan NN, Aksoy M. A review of self-seeded RSOA based on WDM PON. Canad J Electr Comput Eng 2019;42:2–9.
[9] Ghazi A, Aljunid S, Noori A, Idrus SZS, Rashidi C, Al-Dawoodi A. Design & investigation of 10 × 10 gbit/s MDM over hybrid FSO link under different weather conditions and fiber to the home. Bull Electr Eng Inform 2019;8:121–6.
[10] Maraha H, Ameen KA, Mahmood OA, Al-dawoodi A. DWDM over FSO under the Effect of Different Atmospheric Attenuations. Indones J Electr Eng Comput Sci 2020;18:1089–95.
[11] Alshwani S, Fakhrudeen AM, Ismael MN, Al-Dawoodi A, Ghazi A. Hermite-Gaussian mode in spatial division multiplexing over fso system under different weather condition based on linear gaussian filter. Int J Mech Eng Technol 2019;10:1095–105.
[12] Sharma R, Dewra S, Rani A. Performance analysis of hybrid PON (WDM-TDM) with equal and unequal channel spacing. J Opt Commun 2016;37:247–52.
[13] Noori A, Amphawan A, Ghazi A, Ghazi SA. Dynamic evolving neural fuzzy inference system equalization scheme in mode division multiplexer for optical fiber transmission. Bull Electr Eng Inform 2019;8:127–35.
[14] Bai N, Ip E, Huang YK, Mateo E, Yaman F, Li MJ, et al. Mode-division multiplexed transmission with inline few-mode fiber amplifier. Opt Express 2012;20:2668–80.
[15] Essiambre R-J, Kramer G, Winzer PJ, Foschini GJ, Goebel B. Capacity limits of optical fiber networks. J Light Technol 2010;28:662–701.
[16] Zhou Z, Zhang H, Chun L, Sharma A. Performance Analysis of Duobinary and CSRZ Modulation Based Polarization Interleaving for High-Speed WDM-FSO Transmission System. J Opt Commun 2022;43(1):147–52.
[17] L. Li and A. Sharma. "High speed rgb-based duobinary-encoded visible light communication system under the impact of turbulences," *Front. Phys.*, vol. 10, article no. 944623, 2022.
[18] Sharma A, Malhotra J. Performance enhancement of photonic radar sensor for detecting multiple targets by incorporating mode division multiplexing. Opt Quant Electron 2022;54(7).
[19] Sharma A, Malhotra J. Simulative investigation of FMCW based optical photonic radar and its different configurations. Opt Quant Electron 2022;54(4).
[20] Singh H, Mittal N. Performance analysis of free space optical communication system under rain weather conditions: A case study for inland and coastal locations of India. Opt Quant Electron 2021;53:1–21.
[21] Li G, Bai N, Zhao N, Xia C. Space-division multiplexing: The next frontier in optical communication. Adv Opt Photonics 2014;6:413–87.
[22] Xie G, Li L, Ren Y, Huang H, Yan Y, Ahmed N, et al. Performance metrics and design considerations for a free-space optical orbital-angular momentum–multiplexed communication link. Optica 2015;2(4):357.
[23] Yao AM, Padgett MJ. Orbital angular momentum: Origins, behavior and applications. Adv Opt Photonics 2011;3:161–204.
[24] El-Mottaleb SAA, Singh M, Chehri A, Ahmed HY, Zeghid M, Khan AN. Capacity Enhancement for Free Space Optics Transmission System Using Orbital Angular Momentum Optical Code Division Multiple Access in 5G and beyond Networks. Energies 2022;15:7100.
[25] Phillips RL, Andrews LC. Spot size and divergence for Laguerre Gaussian beams of any order. Appl Opt 1983;22:643–4.
[26] Willner AE, Pang K, Song H, Zou K, Zhou H. Orbital angular momentum of light for communication. Appl Phys Rev 2021;8:041312.
[27] Li H, Phillips DB, Wang X, Ho Y-L-D, Chen L, Zhou X, et al. Orbital angular momentum vertical-cavity surface-emitting *lasers*. Optica 2015;2:547–52.
[28] Van Kerrebrouck J, Pang X, Ozolins O, Lin R, Udalcovs A, Zhang L, et al. High-speed pam4-based optical sdm interconnects with directly modulated long-wavelength vcsel. J Lightw Technol 2019;37:356–62.
[29] Murugan KHS. Design and analysis of 5G optical communication system for various filtering operations using wireless optical transmission. Res Phys 2019;12:460–8.
[30] Nguyen D, Bohata J, Komanec M, Zvanovec S, Ortega B, Ghassemlooy Z. Seamless 25 GHz transmission of LTE 4/16/64-QAM signals over Hybrid SMF/FSO and wireless link. J Light Tech 2019;37:6040–7.
[31] Kumari M, Sharma A, Chaudhary S. High-Speed Spiral-Phase Donut-Modes-Based Hybrid FSO-MMF Communication System by Incorporating OCDMA Scheme. Photonics 2023;10:94.
[32] Allen L, Beijersbergen MW, Spreeuw RJC, Woerdman JP. Orbital angular momentum of light and the transformation of Laguerre-Gaussian laser modes. Phys Rev A 1992;45:8185–9.

[33] Wang, J.; Liu, J.; Lv, X.; Zhu, L.; Wang, D.; Li, S.; Wang, A.; Zhao, Y.; Long, Y.; Du, J.; et al. Ultra-high 435-bit/s/Hz spectral efficiency using N-dimentional multiplexing and modulation link with pol-muxed 52 Orbital Angular Momentum (OAM) modes carrying Nyquist 32-QAM signals. In Proceedings of the European Conference on Optical Communication (ECOC 2015), Valencia, Spain, 27 September–1 October 2015.
[34] Zhao L, Liu H, Hao Y, Sun H, Wei Z. Effects of atmospheric turbulence on OAM-POL-FDM hybrid multiplexing communication system. Appl Sci 2019;9:5063.
[35] Willner AE, Huang H, Yan Y, Ren Y, Ahmed N, Xie G, et al. Optical communications using orbital angular momentum beams. Adv Opt Photonics 2015;7:66–106.
[36] D.M. Fatkhiev, M.A. Butt, E.P. Grakhova, R.V. Kutluyarov, I.V. Stepanov, N.L. Kazanskiy, S.N. Khonina, V.S. Lyubopytov, A.K. Sultanov, "Recent Advances in Generation and Detection of Orbital Angular Momentum Optical Beams—A Review," *Sensors* vol. 21, article 4988, 2021.
[37] Dwivedi R, Sharma P, Jaiswal VK, Mehrotra R. Elliptically squeezed axicon phase for detecting topological charge of vortex beam. Opt Commun 2021;485:126710.
[38] Xie G, Ren Y, Yan Y, Huang H, Ahmed N, Li L, et al. Experimental demonstration of a 200-Gbit/s free-space optical link by multiplexing Laguerre-Gaussian beams with different radial indices. Opt Lett 2016;41:3447–50.
[39] Shakthi Murugan KH, Sharma A, Malhotra J. Performance analysis of 80 Gbps Ro-FSO system by incorporating hybrid WDM-MDM scheme. Opt Quant Electron 2020;vol. 52, article no. 505.
[40] Singh M, Atieh A, Grover A, Barukab O. Performance analysis of 40 Gb/s free space optics transmission based on orbital angular momentum multiplexed beams. Alexandria Eng J 2022;61:5203–12.
[41] Muhammad, S.S.; Kohldorfer, P.; Leitgeb, E. Channel modeling for terrestrial free space optical links. In Proceedings of the 2005 7th International Conference Transparent Optical Networks, Barcelona, Spain, 7 July 2005; Volume 1, pp. 407–410.
[42] Singh H, Mittal N, Miglani R, Singh H, Gaba GS, Hedabou M. Design and analysis of high-speed free space optical (FSO) communication system for supporting fifth generation (5G) data services in diverse geographical locations of India. IEEE Photonics J 2021;13:1–12.
[43] Singh M, Atieh A, Aly M, El-Mottaleb SAA. 120 Gbps SAC-OCDMA-OAM-based FSO transmission system: Performance evaluation under different weather conditions. Alex Eng J 2022;61:10407–18.
[44] Mirza J, Ghafoor S, Hussain A. A full duplex ultrawideband over free-space optics architecture based on polarization multiplexing and wavelength reuse. Microw Opt Technol Lett 2020;62:3999–4006.
[45] Naila, C.B.; Bekkali, A.; Kazaura, K.; Matsumoto, M. Bpsk intensity modulated free-space optical communications using aperture averaging. In Proceedings of the International Conference on Photonics 2010, Langkawi, Malaysia, 5–7 July 2010; pp. 1–5.
[46] Kaushal H, Jain V, Kar S. Free-space optical channel models. In: Free Space Optical Communication. Optical Networks. New Delhi, India: Springer:; 2017. p. 41–89.
[47] Luong DA, Thang TC, Pham AT. Effect of avalanche photodiode and thermal noises on the performance of binary phase-shift keying-subcarrier-intensity modulation/free-space optical systems over turbulence channels. IET Commun 2013;7:738–44.
[48] Abd El-Mottaleb SA, Singh M, Ahmed HY, Zeghid M, Nisar KS, Alotaibi MF, et al. Performance evaluation of a 160-Gbit/s OCDMA-FSO system via Laguerre-Gaussian beams under weather conditions. Alex Eng J 2023;63:661–74.
[49] Feng J, Zhao X. Performance analysis of ook-based fso systems in gamma-gamma turbulence with imprecise channel models. Opt Commun 2017;402:340–8.